Polar Biosci., **20**, 1–20, 2006

Frontal positions and mixed layer evolution in the Seasonal Ice Zone along 140°E in 2001/02

Shigeru Aoki[1*], Stephen R. Rintoul[2], Hiroshi Hasumoto[3] and Hideki Kinoshita[4]

[1]*Institute of Low Temperature Science, Hokkaido University, Kita-19, Nishi-8, Kita-ku, Sapporo 060-0819*
[2]*CSIRO Marine and Atmospheric Research and Antarctic Climate and Ecosystems Cooperative Research Centre, GPO Box 1538, Hobart, Tasmania 7001, Australia*
[3]*Oceanographic Research Institute, The University of Tokyo, Minamidai, Nakano-ku, Tokyo 164-8639*
[4]*Hydrographic and Oceanographic Department, Japan Coast Guard, 5–3–1, Tsukiji, Chuo-ku, Tokyo 104-0045*
[*]*Corresponding author. E-mail: shigeru@lowtem.hokudai.ac.jp*

(Received November 28, 2005; Accepted August 9, 2006)

Abstract: We describe the circulation and seasonal development of the upper ocean in the Seasonal Ice Zone (SIZ) of the Southern Ocean along 140°E. The 140°E section was repeated four times between November 2001 and March 2002, spanning the period from early spring to autumn. The sea ice edge was located at 62°–63°S in November, and retreated to 65°S in January. The circulation in the region is dominated by several fronts: the southern branch of Polar Front (PF-S) was located between 60° and 61.5°S; the northern branch of Southern ACC front (sACCf-N) was located at 61.5°–63°S, and roughly corresponds with the winter sea ice edge; and the southern branch of sACCf, the southern boundary of the ACC, and the Antarctic Slope Front (ASF) were closely spaced and found between 64°S and 65°S. Vigorous cyclonic (clockwise) eddies were identified in the region between the sACCf-N and sACCf-S throughout the period.

Changes in salinity made the dominant contribution to changes in density in the SIZ, while changes in temperature made the largest contribution to density changes in the AZ, north of the sACCf. The depth of the mixed layer generally shoaled to the south, in all seasons. The decrease in mixed layer depth occurred in a series of steps. Seasonal variability in the depth of the mixed layer was strongest in the AZ, where summer warming formed a strong seasonal thermocline above the relatively deep (100 m) Winter Water layer. In the SIZ, the mixed layer became warmer, fresher and lighter in summer but the depth of the mixed layer remained at about 50 m throughout the year. The freshest surface waters were observed in the SIZ in January, immediately following the melt and retreat of the sea ice pack. An increase in mixed layer salinity from January to March likely reflects the effect of mixing with saltier waters below the mixed layer. Mixed layer depths south of the ASF were highly variable, both within and between seasons, varying from a minimum of ~20 m in January to over 500 m in March.

key words: Seasonal Ice Zone, Antarctic Circumpolar Current, mixed layer, cyclonic eddies

Introduction

Understanding of primary production and carbon export in the Southern Ocean remains relatively poor, due to a lack of observations. In particular, most measurements

have been made in summer and there is little information on the seasonal evolution of the upper layers of the Southern Ocean. The seasonal cycle of atmosphere–ocean–sea ice interaction can influence biological production by altering the light and nutrient environment through changes in stratification, upwelling and mixing. Horizontal advection may also play a role by redistributing organisms. Here we describe the seasonal evolution of the upper ocean along 140°E using observations from a four-ship survey conducted between early spring (November 2001) and autumn (March 2002), with a focus on the seasonal ice zone.

The dominant circulation features in the region are several fronts of the Antarctic Circumpolar Current (*e.g.*, Orsi *et al*., 1995; Belkin and Gordon, 1996; Rintoul *et al*., 1997; Rintoul and Bullister, 1999; Sokolov and Rintoul, 2002). The fronts often coincide with water mass or biogeographic boundaries. At 140°E, the fronts south of 60°S include the southern branch of the Polar Front (S-PF), the southern and northern branches of the southern ACC front (sACCf-N and sACCf-S), and the Southern Boundary (SB) of the ACC. South of the ACC on the continental slope around Antarctica, the westward flowing Antarctic Slope Front (ASF) divides the cold coastal water from offshore (Gill, 1973; Ainley and Jacobs, 1981; Whitworth *et al*., 1998).

Observations of the seasonal evolution of the mixed-layer are still limited in the Southern Ocean. Rintoul *et al*. (1997) describe the seasonal development of the mixed-layer using WOCE (World Ocean Circulation Experiment) and SURVOSTRAL (SURVey of the Ocean South of ausTRALia) data. They showed heat convergence in summer season in the latitudinal band between 54°S and 62°S. Trull *et al*. (2001) reconstructed seasonal cycles of the mixed-layer from WOCE cruises from different years. Chaigneau *et al*. (2004) extended the above results both in temporal and spatial extent and described the seasonal and interannual variations of the mixed layer. However, these studies were mainly limited to the Antarctic Zone (AZ) region north of the Seasonal Ice Zone (SIZ) and were reconstructed using sections from different years.

To understand the seasonal variations of the near surface process and their influence on biological and biogeochemical cycles in the SIZ of the Southern Ocean off the Adélie Coast, time series observations were made by four vessels in the 2001/02 season (Odate *et al*., 2001; Fukuchi *et al*., 2002). This study is unusual, in that the seasonal changes are documented using repeated CTD observations from a single spring-autumn period, thus avoiding aliasing of interannual variability. We use the repeat sections to describe the frontal structure, circulation and mixed layer evolution, focusing on the SIZ. A primary aim of the paper is to provide the physical context for a variety of biology and biogeochemistry studies carried out on the repeat cruises.

Observations

In-situ observations

As part of a joint Japanese–Australian experiment, four sections were completed along 140°E between early spring and early autumn in the 2001/02 period (Odate *et al*., 2001; Fukuchi *et al*., 2002). The sections extended from 60°S to the continental shelf (Fig. 1).

Aurora Australis observations were conducted as CLImate VARiability and its pre-

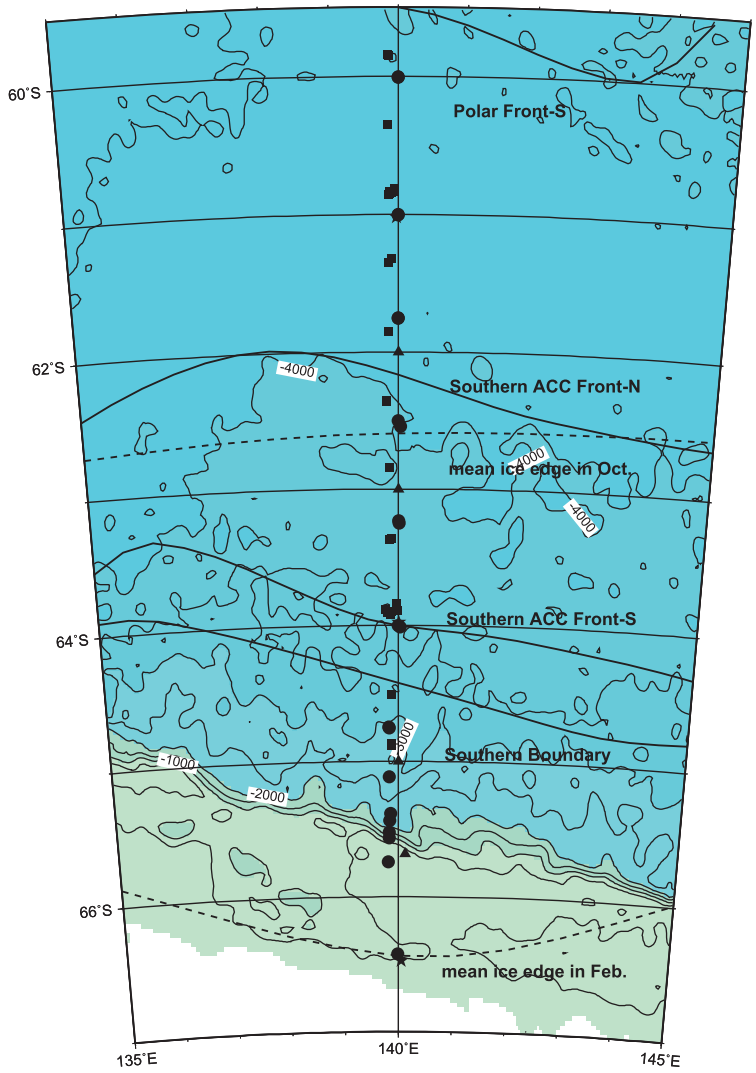

Fig. 1. Observation locations along 140°E in the 2001/2002 season. Squares denote Aurora CTD observations, triangles *Hakuho-maru*, circles *Tangaroa*, and stars *Shirase* observations, respectively. Thick lines denote the fronts derived from Sokolov and Rintoul (2002). Broken lines denote the climatological sea ice edge in October and February.

dictability (CLIVAR) SR3 cruise in November–December 2001. CTD observations were conducted with a General Oceanics Mark IIIC (WOCE upgraded) unit (Rosenberg *et al*., 2005), with a station spacing of 0.5 degrees of latitude. We use stations from 60.8°S to 63.8°S, occupied between November 21–25. The southern-most two stations (64.9°S and 64.5°S) were occupied on the return to Hobart on December 4–5. The sea ice edge was encountered at about 63.5°S. Shallow casts down to a few hundred meter depths were

completed at some stations as well as the routine top-to-bottom observations.

Hakuho-maru occupied the section in January 2002 with Seabird SBE 911 CTD units. Observations were generally conducted with a spacing of one degree. CTD cast was done at 65°S on January 8, and then observation was conducted at 65.7°S on January 10. Subsequent observations were completed between 64°S on January 12 and 60°S on January 15.

Tangaroa's survey was completed in February. The SBE 911 CTD units were used (Aoki and Sato, 2004). Observations were conducted as the 43rd Japanese Antarctic Research Expeditions–STudies of Antarctic oceans and Global Environment (JARE-43 –STAGE). Spatial sampling was 0.75° in general, with closer station spacing over the continental slope region. The southern-most station (66.4°S) was occupied on February 13. Observations were then made at 64°S on February 15. On the way to the southern station at 65.8°S on February 18, a few stations were occupied and then the station at 60°S was finally completed on February 27. Shallow casts were deployed for eleven stations as well as the routine top-to-bottom casts.

As the last of this sequence, *Shirase* finished observations in March with Falmouth Scientific Inc. TRITON ICTD units. Observations were conducted under the auspices of JARE-43 (Kinoshita and Nosaka, 2005). Three stations were occupied northward at 66.4°S on March 9, at 64°S on March 10, and at 61°S on March 11. Temperature and salinity observations with Tsurumi XCTD were supplemented for the derivation of the frontal positions to fill in the large gaps in-between the CTD stations.

Throughout these cooperative observations, three stations at 61°S, 64°S, and 66.4°S were set as common stations to represent different regional structure. For *Aurora Australis* and *Tangaroa*, data from routine top-to-bottom casts were used mainly, but the shallow casts were also used to estimate short-term variations of the mixed-layer properties.

In the remainder of the paper, we refer to the *Aurora Australis*, *Hakuho-maru*, *Tangaroa*, and *Shirase* sections as the November, January, February and March sections, respectively.

Satellite observations

Satellite data were used to investigate the spatial structure of the oceanic and sea ice conditions. Daily maps from the Special Sensor for Microwave Imager (SSM/I) were used to derive sea ice concentrations and the positions of the sea ice edge. The NASA Team algorithm was applied to the dataset used (Cavalieri *et al*., 1990; Comiso, 1990–2000). Weekly maps of sea surface height and geostrophic current anomalies from altimetry data were used to infer the spatial patterns of the surface current. CNES/NASA TOPEX/POSEIDON data and CLS "SLA" and "MSLA" products were used (Le Traon *et al*., 1998). Climatological temperature and salinity distributions of the WHP-SAC (Gouretski and Jancke, 1998) were used to construct the mean dynamic height and geostrophic current field.

Sea ice condition in the study region

The evolution of sea ice concentrations from SSM/I is shown in Fig. 2. In early November, the sea ice edge was located between 62°S and 63°S, and by mid-November, the

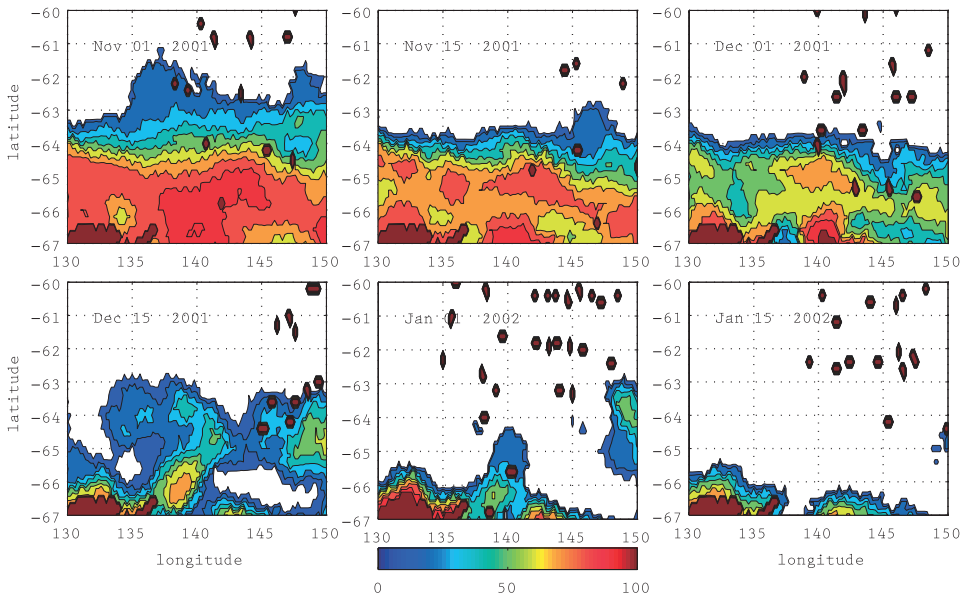

Fig. 2. Sea ice distribution (compactness) in the study region. Contour interval is 10% concentration.

ice edge had retreated to about 63.5°S. The ice edge did not move much over the following fortnight, although ice concentration within the pack declined significantly. Higher resolution satellite images showed that the ice edge was accompanied by clockwise eddy-like features in early December (Hirawake *et al.*, 2003; Aoki *et al.*, 2006). By mid-December, the coastal area between 140°E and 150°E became sea ice free, and ice concentrations within the pack declined further, while the sea ice edge extended northward by about a degree of latitude. The retreat of the sea ice was very rapid after mid-December, leaving the region nearly ice-free by mid-January. As described below, the input of sea ice melt in late December–early January had a significant influence on the mixed layer in the SIZ.

Front positions

The dominant circulation features in the region are associated with fronts of the ACC. Along 140°E, several fronts have been identified south of 60°S (Sokolov and Rintoul, 2002): the S-PF, sACCf-N and sACCf-S, and SB. To the south of the ACC, the ASF is located over the continental slope. Using a series of repeat hydrographic sections along 140°E, Sokolov and Rintoul (2002) derived temperature-based criteria that could be used to reliably identify each of the fronts (Table 1). Here we use water mass properties, the temperature criteria, and geostrophic currents to locate the fronts.

Water mass properties and the fronts

The fronts generally represent boundaries between zones with similar water mass

Table 1. Fronts and their indicators along 140°E line.

Front	Criteria
PF-S	θ>2.2°C at θ max
SACC-N	θ>2.0°C at θ max
SACC-S	θ>1.8°C at θ max
SB	θ>1.5°C at θ max
ASF	θ=0°C at p=200 dbar

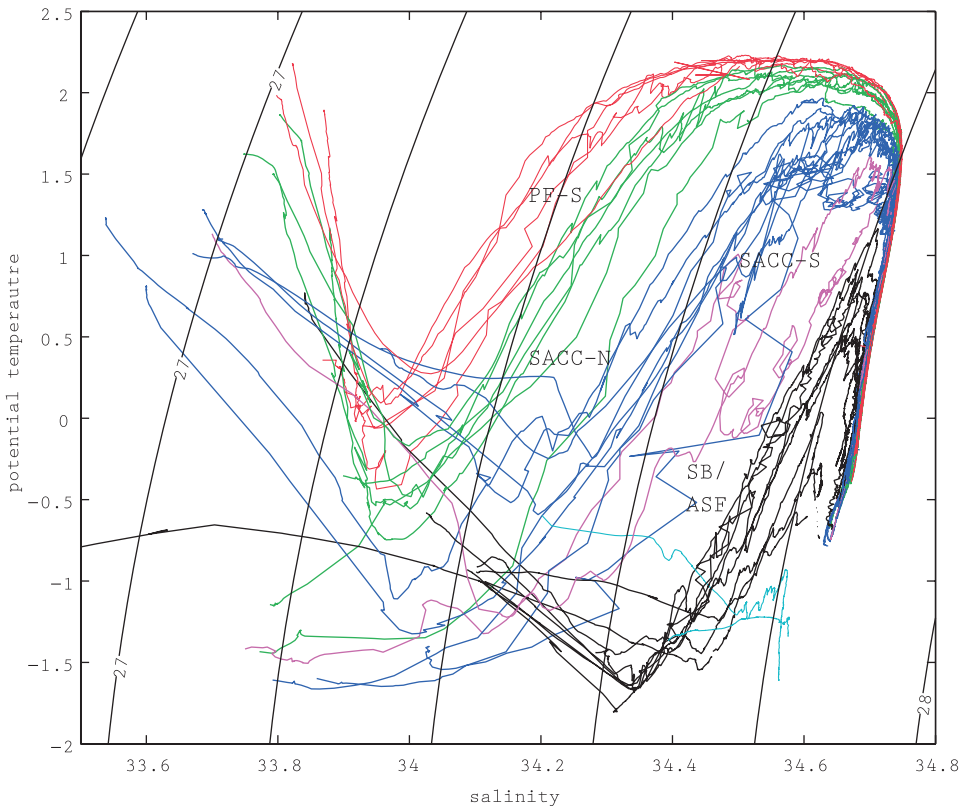

Fig. 3. Potential temperature-salinity diagram for all top-to-bottom CTD data. Red lines denote the data from the northern branch of Polar Front (PF-N) to the southern branch of PF (PF-S), green lines from PF-S to the northern branch of southern ACC front (SACC-N), blue from SACC-N to Antarctic Slope Front (ASF), black south of ASF, and cyan near the coast, respectively. Magenta lines denote those in the cyclonic eddies.

properties and therefore correspond to gaps between clusters of similar profiles on the potential temperature-salinity (T-S) diagram (Fig. 3). The major water masses correspond to the following regions of the T-S diagram, starting in the deep ocean: the end of the

T-S curves with temperature less than 0°C and salinity greater than 34.64 is Antarctic Bottom Water; the overlying salinity maximum in the upper right corner marks the core of the Lower Circumpolar Deep Water; and the temperature minimum consists of Winter Water, the remnant of the winter mixed layer. The warmer and fresher water found between the temperature minimum and the sea surface is known as Antarctic Surface Water. Water lying above the salinity maximum generally migrates from the upper-left (warm/fresh) to the lower-right (cool/saline) side of the diagram, when moving from north to south.

Using the criteria in Table 1, the positions of the fronts were derived for each CTD section (Table 2). The front positions inferred in this way agreed closely with those inferred from the "gaps" in the T-S diagram. The S-PF and sACCf-N were clearly identified and distinct from the other fronts. The S-PF was located at 60°–61.5°S for all sections. The sACCf-N was located at 61.5°–63°S. The sACCf-N roughly corresponds to the maximum extent of the winter sea ice edge (Fig. 1). While the above two fronts were clearly identified, the fronts from the sACCf-S to ASF were closely spaced in a narrow band between 64°S and 65°S and could not be individually resolved by the station spacing.

The progression from upper left to lower right of the T-S diagram with increasing latitude is interrupted by anomalous profiles observed in November, February, and March. The water properties at these stations between 62°S and 64°S are similar to those found further south over the continental slope. As discussed below, these profiles are from cold-core eddies observed between the sACCf-N and sACCf-S on the three sections.

To the south of the ASF, a rapid change in subsurface water properties occurred over a distance of only 3 nautical miles between 65.5°S and 65.6°S in February. The water

Table 2. Positions and indicators of fronts along 140°E line. Each pair of values gives the latitude (top line) and temperature (bottom line) of the stations bracketing each front.

Cruise	November *Aurora*	January *Hakuho-maru*	February *Tangaroa*	March *Shirase*
PF-S (°S)	61.3–60.8	61.0–60.0	61.0–60.0	61.3–61.0
2.2°C (θ max)	2.17–2.20	2.15–2.21	2.15–2.23	(2.16)–2.21
SACC-N (°S)	62.8–62.4	63.0–62.0	62.5–61.8	62.5–62.1
2.0°C (θ max)	1.44–2.10	1.90–2.10	1.97–2.12	(1.92)–(2.07)
SACC-S (°S)	64.5–63.8	65.0–64.0	64.8–64.0	64.5–63.2
1.8°C (θ max)	1.62–1.92	1.16–1.83	1.73–1.82	(1.44)–(1.82)
SB (°S)	64.9–64.5	65.0–64.0	65.1–64.8	64.5–64.0
1.5°C (θ max)	0.77–1.62	1.16–1.83	0.91–1.73	(1.44)–1.79
ASF (°S)	64.9–64.5	65.0–64.0	65.1–64.8	65.3–65.1
0°C (200 db)	−0.70–1.34	−0.21–1.79	−1.29–1.66	(−0.40)–(0.31)

Numbers in parentheses denote the XCTD temperature.

mass change is evident as a large gap for subsurface waters in the T-S diagram between colder water over the shelf and warmer water just offshore (among black curves in Fig. 3), while surface water masses are similar at both locations. A similar rapid transition was observed at the same position for SR3 au9407 cruise in January 1994. South of the shelf break near 300 m depth at 65.5°S, the bottom depth deepens shoreward to values greater than 1000 m. The southern-most stations by *Tangaroa* and *Shirase* were occupied in this depression, where the water was cooler than −0.5°C throughout the water column.

Geostrophic currents and the fronts

Geostrophic currents relative to the 2500 dbar level were derived for the ACC region (Fig. 4). Eastward current maxima over 0.05 m/s were found at about 60.5°S, 62°S, and 64°–65°S in November. In January, eastward maxima were also found at 61°–62°S and 64°–65°S, although the spatial sampling was rather sparse. In February, eastward maxima were found at almost the same locations as found in November. In each case, the position of the geostrophic transport maxima coincide with the front positions inferred from the water mass properties. Westward flow was found at 63.5°S in November and February. The position corresponds to the southern side of the cold-core eddy discussed above. Schematic positions of the fronts and the eddy-like features are summarized in Fig. 5, as inferred from the temperature indicators and geostrophic currents.

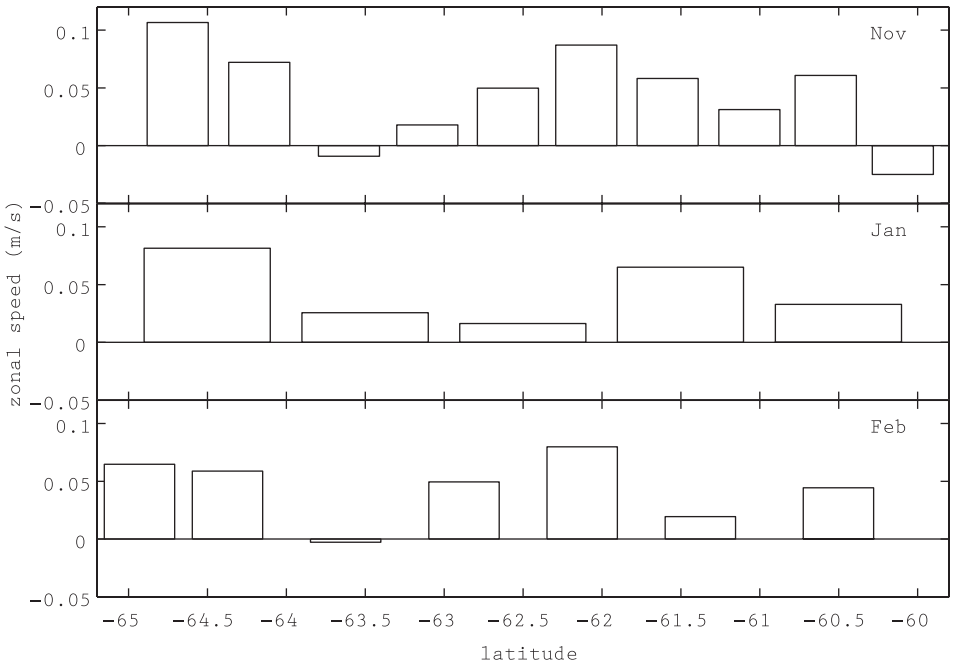

Fig. 4. Zonal geostrophic current relative to 2500 dbar for November 2001–February 2002.

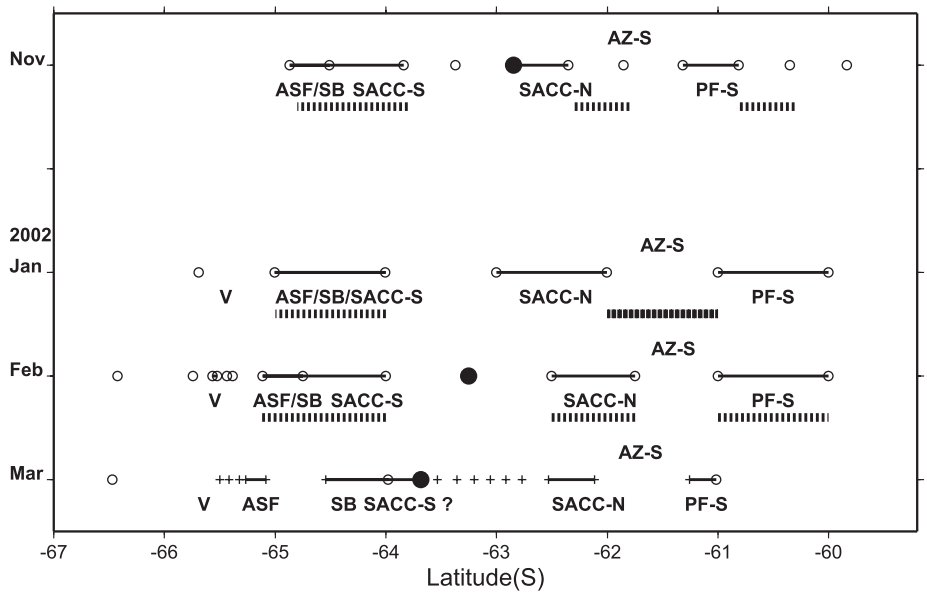

Fig. 5. Schematic location of fronts with observation points for the 140°E sections. Open circles denote CTD observation points and crosses XCTD points. Lines were derived from temperature indicators and broken lines from geostrophic current. Large dots denote the latitudes of the eddy-like features.

Mixed-layer evolution

Seasonal evolution of water mass properties

The overall water mass structure and seasonal evolution of the upper ocean along 140°E is illustrated using vertical sections of potential temperature, salinity and potential density (Fig. 6). At depth, the relatively warm and saline Circumpolar Deep Water shoals from north to south across each section. The shoaling of isopycnals below the mixed layer reflects both the tilt of isopycnals across the geostrophic fronts of the ACC and the upwelling driven by divergent Ekman transport (*i.e.* the Antarctic Divergence). The cooler and fresher waters above the salinity maximum vary strongly with season.

In November, the relatively cold and deep surface mixed layer and the absence of a subsurface temperature minimum indicate that the section represents late winter–early spring conditions (*i.e.* before significant summer warming has occurred). By January, warming of the surface layer has produced a warm, shallow mixed layer above the pronounced temperature minimum that is the remnant of the previous winter. Further warming during February enhances the sharp seasonal thermocline above the temperature minimum. The surface mixed layer is distinctly fresher in January and February than in November, reflecting the melting of sea ice. The warming and freshening of the surface layer causes a decrease in density. Note also the presence of the cold core eddy between 62°S and 64°S in the November and February sections.

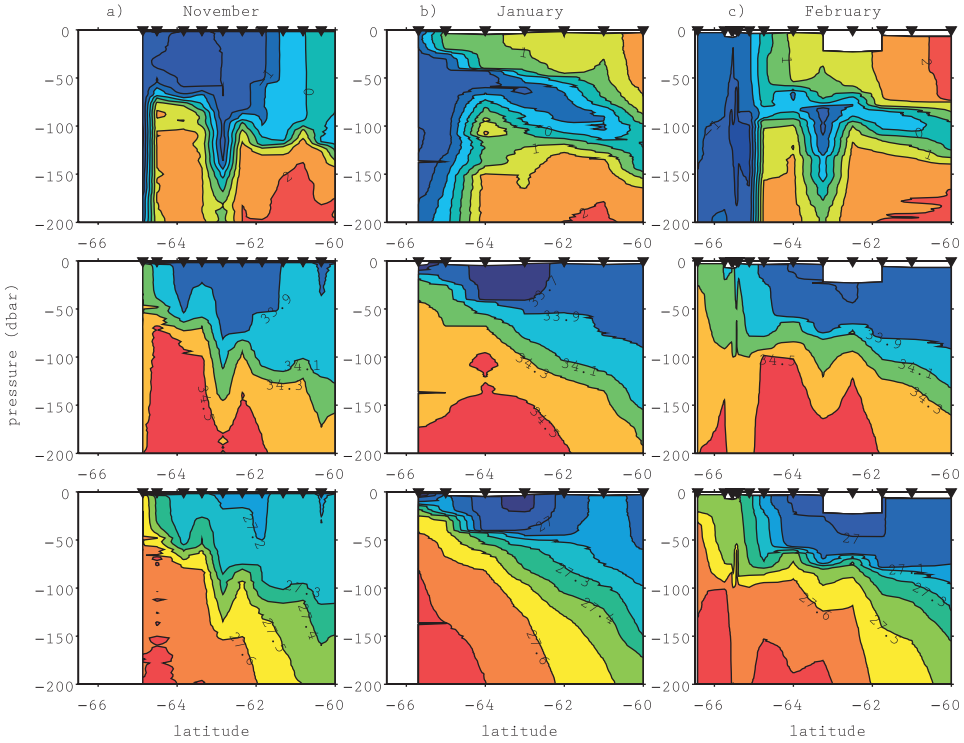

Fig. 6. Vertical sections of potential temperature (upper panel), salinity (middle), and sigma 0 (lower) for the section in November (a), January (b), and February (c). Triangles denote observation points.

Differences in the seasonal evolution of the SIZ and AZ can be seen more easily in the meridional distribution of the surface temperature, salinity, and potential density (Fig. 7). Surface temperature generally decreases poleward. Surface salinity also decreases poleward as far as the sACCf-S at 64°S, then increases further south. The southward increase in salinity likely reflects the effect of brine rejection during sea ice formation in winter, and the effect of ice drift causing net formation in the south and net melting further north (Trull *et al*., 2001). Salt input by upwelling of saline Circumpolar Deep Water may also contribute. The distribution of density with latitude in summer is similar to that of salinity, first decreasing, then increasing, from north to south.

Most of the ~2°C warming of the surface layer occurs between November and January, with little additional warming as the season progresses. Seasonal changes in salinity are relatively small north of 62°S (in the AZ), and the summer decrease in density there is largely the result of summer warming. South of 62°S, in the SIZ, the surface salinity decreases rapidly between November and January, as the sea ice melts and retreats, with the largest changes seen at the southern end of the section. However, by February the surface salinity increased again, strongly south of the ASF and more modestly between 62°S and 64°S. The increase in salinity following the period of rapid melt is likely

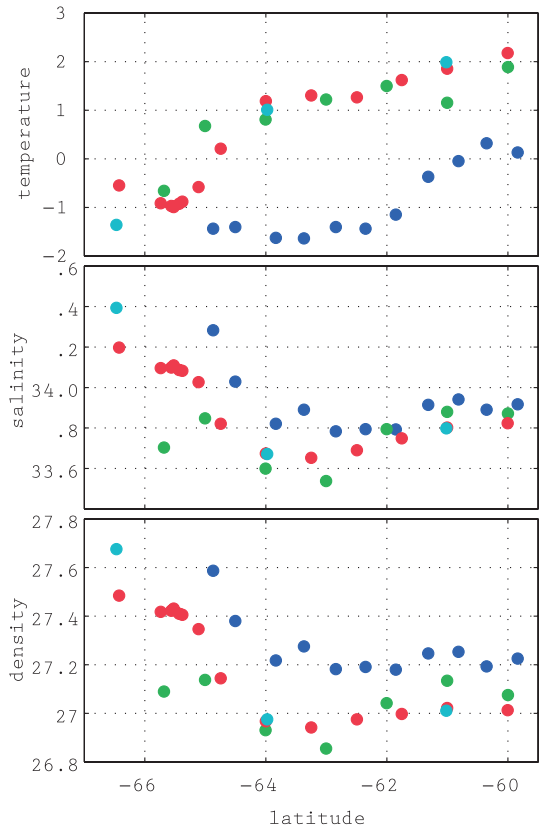

Fig. 7. Meridional distribution of surface potential temperature (upper panel), salinity (middle), and sigma 0 (lower). Blue dots denote November, green January, red February, and cyan March, respectively.

caused by wind-driven mixing of the surface layer entraining saltier water from below, as little sea ice is forming at this time of year (Chaigneau and Morrow, 2002; Chaigneau *et al*., 2004).

Defining the mixed layer depth

Changes in the depth of the mixed layer can be caused by changes in surface forcing (*e.g*. wind stirring, Ekman pumping, and buoyancy forcing) or by changes in heaving of the seasonal thermocline by internal waves. The mixed layer depth therefore varies on a range of time and space scales. A series of repeat stations at three locations along the February (*Tangaroa*) transect illustrates the high frequency variability in the mixed layer (Fig. 8). The mixed layer shoals from north to south, but also varies at each location over time-scales of hours or days as the density profile moves vertically through the water column. The high frequency variability typically introduces an uncertainty of 20–30 dbar in the inferred mixed layer depth at each station. In addition,“transient” shallow mixed lay-

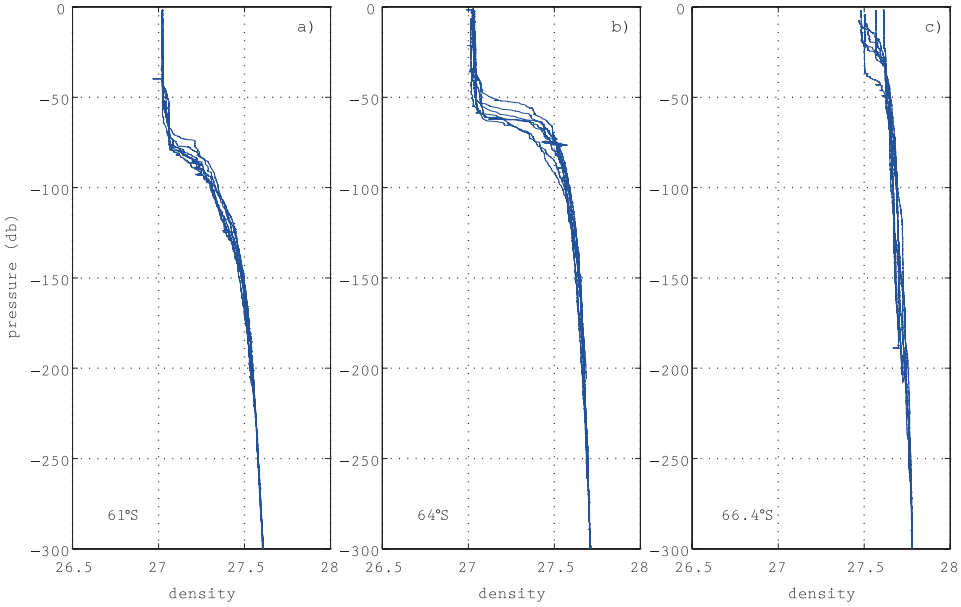

Fig. 8. Vertical profiles of potential density at (a) 61°S, (b) 64°S, and (c) 66.4°S for all available casts in February 2002 (*Tangaroa* cruise).

ers can be formed by changes in surface forcing. For example, a cloud-free and calm day can result in a large warming of the surface layer and a shallow mixed layer; similarly, an input of sea ice melt can have similar effects. These shallow layers are typically removed when the next storm re-mixes the seasonal mixed layer. By altering the light environment experienced by phytoplankton, such short-term variations in mixed layer depth may have important biological effects.

Here our focus is on the seasonal evolution of the mixed layer, rather than on the transient features. A number of indicators based on density, temperature, or dissolved oxygen have been used to define the mixed layer depth (*e.g.*, Monterey and Levitus, 1997; Talley, 1999). A commonly used definition of the mixed layer depth is the depth at which the density increases by 0.1 kg m^{-3} from the near-surface value. This simple definition is based on a directly measured parameter (stratification) and has the advantage of using basic variables obtained by standard CTD casts. Inspection of Fig. 8 suggests that this criterion will consistently pick out the depth corresponding to the rapid density increase at the base of the seasonal mixed layer (rather than the more subtle changes in stratification resulting from synoptic forcing). The mixed-layer was thus defined here as the pressure level at which density exceeded the value observed at 10 m by more than 0.1 kg m^{-3}. As the 10 dbar density was not available at 62.5°S for *Tangaroa* cruise, the shallowest available value at 25 dbar was used.

Mixed layer variability

Mixed-layer depths were derived from all the available CTD casts (Fig. 9). For

Aurora and *Tangaroa* cruises, we have multi-cast observations at almost the same location within a day or two. The repeat stations illustrate clearly the short-term variability in the mixed layer depth, which is particularly strong in February at the southern end of the section. Shifts of the strong meridional gradients across the fronts (Fig. 6) may also contribute to the temporal variability observed at a given point.

The mixed-layer depth shoaled from north-to-south, in a series of steps near each front. In November, the mixed layer depth was about 120 dbar to the north of 61.5°S (north of the PF-S), 70 dbar between 62°S and 63°S (between the PF-S and sACCf-N), near 50 dbar between 63°S and 64.8°S (between the sACCf-N and sACCf-S), and greater than 140 dbar south of the ASF. After November, warming and freshening cause the mixed layer depth to shoal, but with a somewhat different seasonal cycle to the north and south of the sACCf-N. To the north, the minimum mixed layer depth of about 80 dbar is reached in February. Further south, within the SIZ, the shallowest mixed layers are found in January, at the time of maximum freshwater release by the melting sea ice. Wind-driven mixing erodes the buoyant surface layer and increases the mixed layer depth by about 20 dbar between January and February. Overall, the seasonal variability in mixed layer depth is at a minimum between the two branches of the sACCf and at a maximum

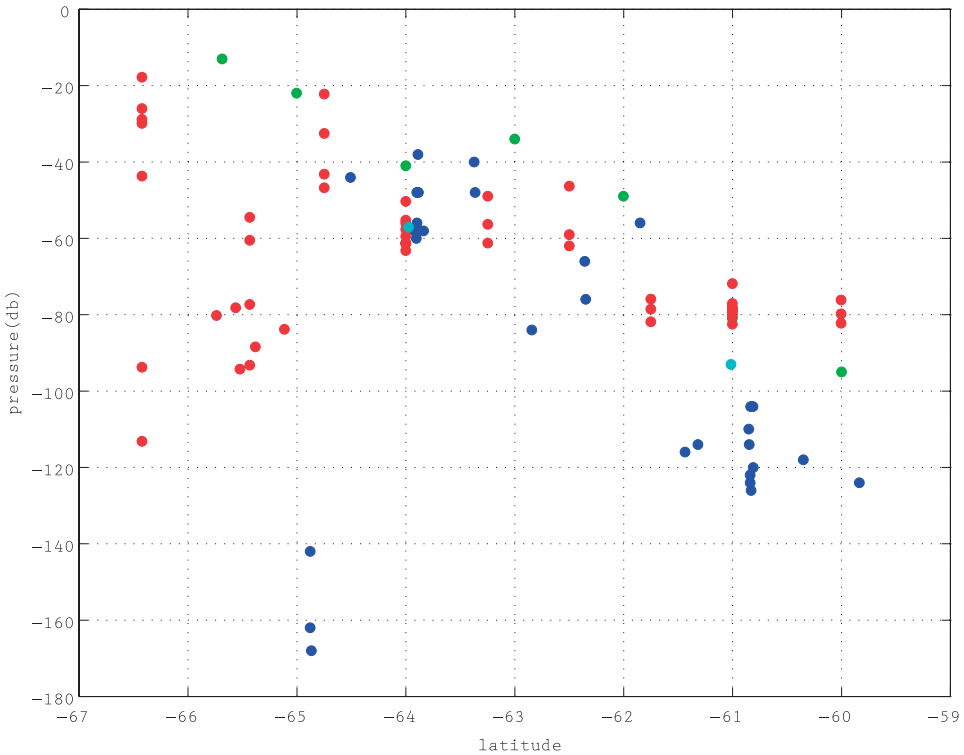

Fig. 9. Meridional distribution of the mixed-layer depths. Blue symbols denote those for November, green for January, red for February, and cyan for March.

over the continental shelf, with more modest seasonal variations observed in the AZ north of the sACCf-N.

The contrasting seasonal development in the AZ, SIZ, and south of the ASF can be seen clearly by comparing repeated stations at 61°S, 64°S, and 66.4°S (Fig. 10). At 61°S in the AZ, the mixed-layer shoaled from 100–120 dbar in November to 70–80 dbar in January–February. The surface layer warmed by 1.4°C and freshened by 0.05 between November and January. There was no sea ice cover in this zone, so local sea ice melting could not occur. The observed freshening is likely due to a combination of northward Ekman transport of fresher surface water from the SIZ and an excess of precipitation over evaporation (Chaigneau *et al.*, 2004). Warming made the dominant contribution to the decrease in surface density of 0.1 $kg\,m^{-3}$; the warming contribution was 0.08 $kg\,m^{-3}$ and the freshening contribution was 0.03 $kg\,m^{-3}$, estimated with the linear approximation. From January to February, there was no significant change in the mixed-layer depth, although warming and freshening of the surface layer continued and the density decreased by another 0.1 $kg\,m^{-3}$. From February to March, surface warming and freshening ceased and the surface mixed-layer deepened to 90 dbar. However, the mixed-layer depth did not yet reach the level of the preceding winter.

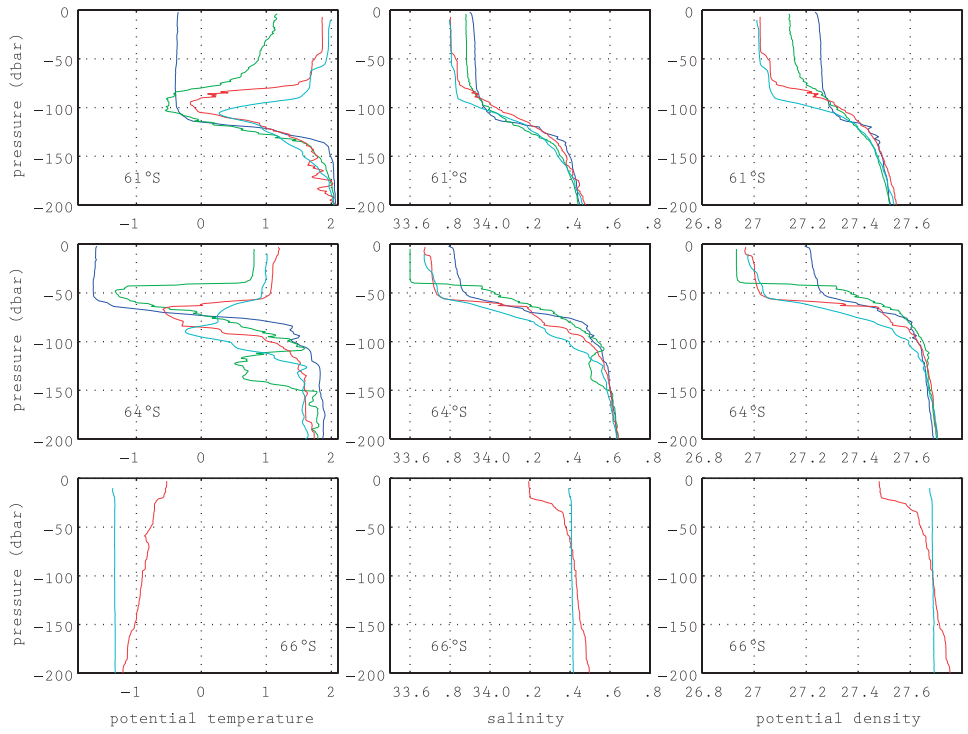

Fig. 10. Seasonal variations in the vertical profiles of potential temperature (left panel), salinity (middle), and sigma 0 (right) at 61°S (upper panel), 64°S (middle), and 66.4°S (lower). Blue lines denote for November, green for January, red for February, and cyan for March.

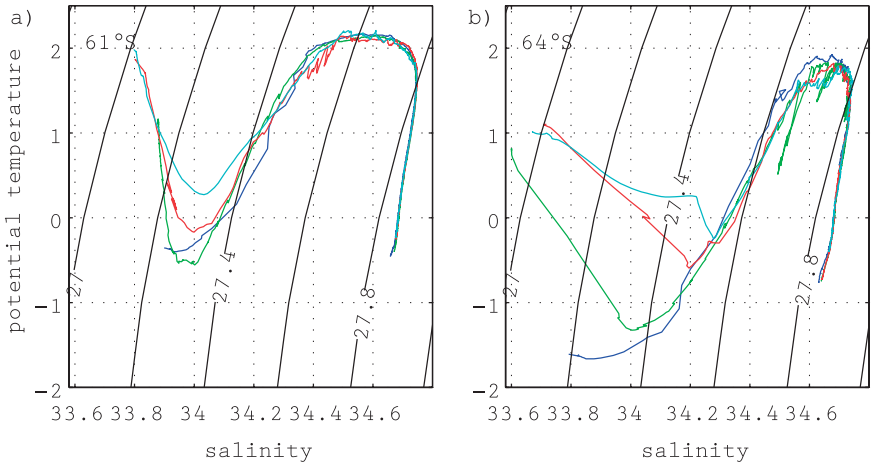

Fig. 11. Potential temperature-salinity diagrams at (a) 61°S and (b) 64°S. Contours denote sigma 0 with the interval of 0.1 kg m^{-3}.

Below the mixed-layer at 61°S, temperature at the temperature minimum layer increased, but the depth of the layer did not change significantly. The T-S diagram clearly shows that the warming (and slight increase in salinity) of the temperature minimum occurred almost along the 27.3 kg m^{-3} surface (Fig. 11). The properties below the temperature minimum did not change significantly.

At 64°S in the SIZ, the mixed-layer was 40–60 dbar deep in November and January (Fig. 10). Salinity decreased sharply by 0.23 from November to January (four times larger than observed at 61°S over the same time period). Sea ice existed until December, so local sea ice melting probably caused this surface freshening. Melting of 0.5 m of sea ice with 0.5 compactness can explain the surface layer freshening down to 40 m. This is a fair assumption from the mean sea ice state in this region (Worby *et al.*, 1998). Surface temperature also increased by 2.4°C due to summer warming. However, the significant salinity change had a much larger effect on the decrease in density of 0.30 kg m^{-3}; the warming contribution was 0.11 kg m^{-3} while the freshening contribution was 0.19 kg m^{-3} (Fig. 11). From January to February, surface salinity and density increased and the mixed-layer deepened by 20 dbar. Mixing with underlying water can cause an increase in the salinity of the surface mixed-layer. Temperature continued to rise during this period, again emphasizing the role of salinity in increasing the surface density. From February to March, surface freshening and slight cooling occurred, but no significant change in mixed-layer depth was observed.

Significant variations in water mass properties are observed below the surface mixed layer at 64°S, in contrast to 61°S. The depth of the temperature minimum deepened from 50 dbar in January to 90 dbar in March (Fig. 10). Below the temperature minimum, temperature, salinity and density decreased. Near the temperature maximum, cold and fresh layers were detected (Fig. 11), reflecting intrusions driven by the strong water mass contrasts across the SB/ASF to the south and the cold eddy to the north of 64°S. Subduction

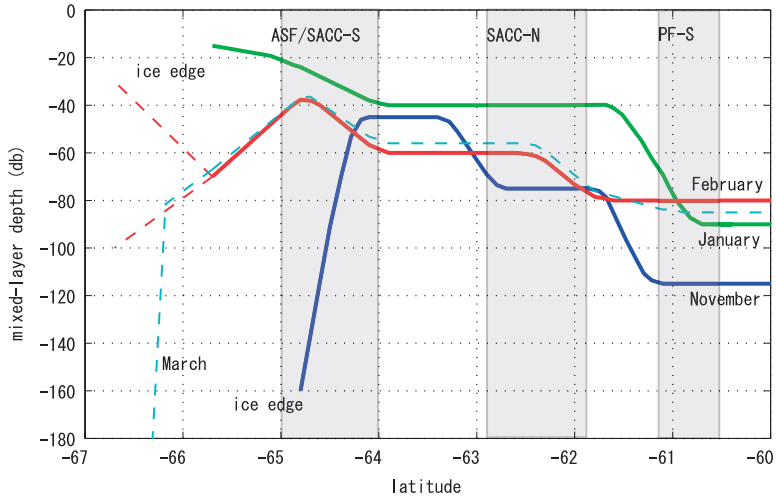

Fig. 12. Schematic seasonal variations of the mixed-layer depths.

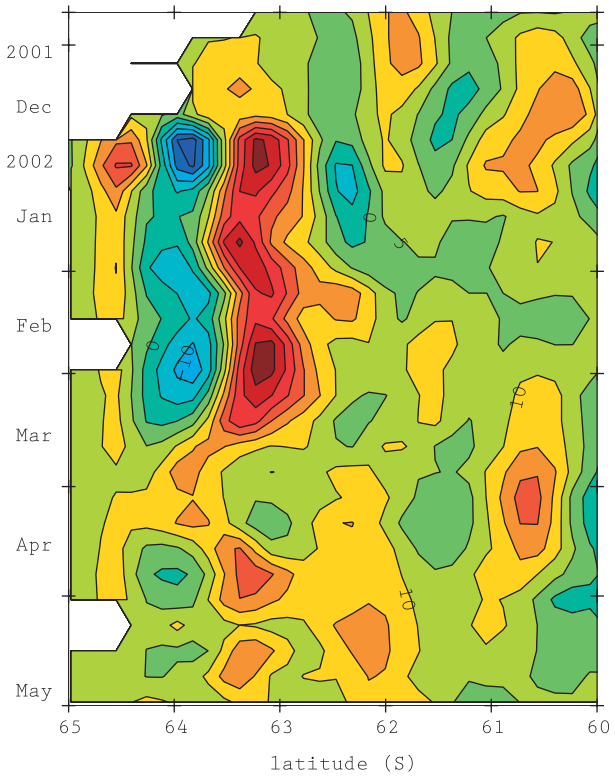

Fig. 13. Zonal geostrophic current at the sea surface derived from TOPEX/Poseidon altimetry.

and northward flow of relatively cold, fresh water from the south may also have contributed to the changes observed below the temperature minimum.

At 66.4°S near the coast, there was sea ice until January and we have observations only in February and March. In February, both shallow (20–40 dbar) and relatively deep (100 dbar) mixed-layers were observed in a single day (Fig. 8c and Fig. 9; the profile in Fig. 10 shows the shallower one). Between February and March, surface salinity increased by 0.2, temperature decreased by about 1°C, density increased by 0.2 $kg\,m^{-3}$, and the mixed layer depth increased to more than 500 dbar (not shown). The changes in water properties and homogenization of the upper water column indicate that sea ice formation, brine rejection and deep convection had begun by March at this location over the continental shelf.

At 65°–66°S on the continental slope, observations are only available in January and February. In January the mixed-layer was very shallow (20 dbar or less). In February, the mixed-layer was much deeper (50–90 dbar) and the surface salinity had increased by 0.2. The salinity increase is likely caused by wind-driven mixing and entrainment of the more saline water below.

The changes in mixed layer depth with season and with latitude are summarized in the schematic diagram in Fig. 12. Historical estimates of the mixed-layer depth from Monterey and Levitus (1997) are nearly uniform at 30–50 m south of 60°S. The climatological mixed layer depths are therefore underestimated compared to the depths obtained in this study. The seasonal mixed-layer evolution at 61°S in the AZ is similar to that described by Trull *et al*. (2001) and Chaigneau *et al*. (2004). Temperature is the major factor that controls the mixed-layer change in the AZ. In contrast, freshwater supply due to local sea ice melting plays an important role in determining the properties and depth of the mixed layer at 64°S in the SIZ.

A time series of geostrophic surface current derived from satellite altimeter data and a mean dynamic height field is shown in Fig. 13. Strong eastward currents are found near 60°–61°S, 61°–62°S, and 64°–65°S throughout the December to May period covered by the observations, corresponding to the major fronts (PF-S, sACCf-N, and sACCf-S/SB, respectively). The strong eastward flow at 63°S and westward flow near 64°S is associated with the cyclonic eddy seen in the vertical sections in Fig. 6. There is a series of cyclonic eddies, with diameters of 100–150 km that were separated by about 150 km (Hirawake *et al*., 2003; Aoki *et al*., 2006). These eddies were traced for nearly two month from spring-summer seasons, possibly every year, and were detected at least from 133°E to 145°E. The similarity of the water properties in the core of the eddies and on the slope region suggests a significant meridional exchange across the Antarctic Divergence. Hence it can cause a significant "patchy" distribution in the various water mass properties and raises caution on detecting the "seasonal" change in this region.

Summary

We described the surface flow field and seasonal development of the mixed-layer in the SIZ of the Southern Ocean along 140°E from November 2001 to March 2002.

Frontal positions were derived from T-S properties, temperature indices and geostrophic currents. Each of the three criteria placed the fronts in similar positions. The

fronts correspond with water mass boundaries (*i.e.* gaps between clusters of similar profiles on the T-S diagram) and with maxima in the geostrophic current. The front locations coincide well with the climatological positions of the sACCf-N (62°–63°S), sACCf-S (64°S), SB (64°–65°S), and ASF (65°S). The PF-S was observed slightly to the south (60°–61.5°S) of its climatological mean position (59°–60°S), which was consistent with a positive anomaly of SSHA on the latitudinal band. Eddy-like features were identified in the region between the sACCf-N and sACCf-S throughout the period.

Spatial variations of the surface water properties were controlled by salinity in the SIZ, while temperature changes were the dominant factor further offshore in the AZ. The surface mixed-layer was twice as deep (100 dbar) in the AZ than in the SIZ (50 dbar). Step-like changes of the mixed-layer depth were clearly observed in November and February, and the discontinuities occurred near the fronts. In the AZ, seasonal development of the mixed-layer density was in phase with the summer warming. The mixed-layer depth was 100–120 dbar in November, 70–80 dbar in January–February, and 90 dbar in March. In the SIZ, the mixed-layer depth was rather stable, lying between 40 and 60 dbar throughout the period. The shallowest mixed-layer depths were observed near the retreating sea ice edge in January, when the input of freshwater from melting ice caused the formation of a shallow, buoyant, fresh layer. Wind mixing eroded the buoyant surface layer between January and February, driving an increase in salinity and depth of the mixed layer.

This study was confined to the period from spring to early autumn. Winter mixing is undoubtedly important in driving vertical transport and redistribution of the various parameters. Winter hydrographic observations are essential to fully resolve the seasonal process, but the logistic difficulties are great. Hence remotely sensed tactics are promising for monitoring the mixed-layer. Mid-depth profiling floats will significantly improve the information on the seasonal and interannual variations in the mixed layer, but sea ice cover is a formidable barrier for the data transmission. Development of cost-effective surface drifters with profiling function will enable sustained observations of the surface mixed-layer. Establishment of the combined observation system of high-quality hydrography with such remotely sensed techniques are keenly needed to reveal the entire development of the mixed-layer process.

Acknowledgments

Collection of *in situ* data were attributed to Mitsuo Fukuchi, Harvey Marchant, and Makoto Terazaki, who brought the Australian–Japanese cooperative observations to fruition. We are grateful for Tsuneo Odate, the cruise leader of *Tangaroa* of JARE-43 and -44.

Sakae Kudoh provided information of drift speeds of sediment trap buoys equipped with GPS. The altimeter products were produced by the CLS Space Oceanography Division as part of the Environment and Climate EU ENACT project (EVK2-CT2001−00117) and with support from CNES. The SSM/I products were provided by NSIDC. The research was supported in part by the Australian government's Cooperative Research Centre program. This study is a contribution to the CSIRO Climate Change Research Program supported by the Department of Environment and Heritage through the Australian

Greenhouse Office. This study was also supported by Grant-in-Aid for Scientific Research (1570001 and 17340138) of the Japanese Government.

References

Ainley, D. and Jacobs, S.S. (1981): Sea-bird affinities for ocean and ice boundaries in the Antarctic. Deep-Sea Res., **28**, 1173–1185.

Aoki, S. and Sato, T. (2004): JARE-43 *Tangaroa* marine science cruise report (Physical oceanography). Nankyoku Shiryô (Antarct. Rec.), **48**, 204–218.

Aoki, S., Fukai, D., Hirawake, T., Ushio, S., Rintoul, S.R., Hasumoto, H., Ishimaru, T., Sasaki, H., Kagimoto, T., Sasai, Y. and Mitsudera, H. (2006): A series of cyclonic eddies in the Antarctic Divergence off Adélie Coast. J. Geophys. Res., revised.

Belkin, I.M. and Gordon, A.L. (1996): Southern Ocean fronts from the Greenwich Meridian to Tasmania. J. Geophys. Res., **101**, 3675–3696.

Cavalieri, D., Gloerson, P. and Zwally, J. (1990-March 2000): DMSP SSM/I daily polar gridded sea ice concentrations, ed. by J. Maslanik and J. Stroeve. Boulder, CO: National Snow and Ice Data Center. Digital media.

Chaigneau, A. and Morrow, R.A. (2002): Surface temperature and salinity variation from Tasmania to Antarctica. J. Geophys. Res., **107** (C12), 8020, doi: 10.1029/2001JC000808.

Chaigneau, A., Morrow, R.A. and Rintoul, S.R. (2004): Seasonal and interannual evolution of the mixed layer in the Antarctic Zone south of Tasmania. Deep-Sea Res. I, **51**, 2047–2072.

Comiso, J. (1990-March 2000): DMSP SSM/I daily polar gridded sea ice concentrations, ed. by J. Maslanik and J. Stroeve. Boulder, CO: National Snow and Ice Data Center. Digital media.

Fukuchi, M., Odate, T. and Kudoh, S. (2002): Marine biological processes in the Antarctic Ocean: its importance to the global environmental change. The 9th international symposium on Antarctic Science, Program and Abstract, KORDI, Korea, 25–26.

Gill, A.E. (1973): Circulation and bottom water production in the Weddell Sea. Deep-Sea Res., **20**, 111–140.

Gouretski, V.V. and Jancke, K. (1998): Technical Report No. 3, WOCE Report No. 162, WHP Special Analysis Centre.

Hirawake, T., Kudoh, S., Aoki, S. and Rintoul, S.R. (2003): Eddies revealed by SeaWiFS ocean color images in the Antarctic Divergence zone near 140°E. Geophys. Res. Lett., **30** (9), 10.1029/2003GL016996.

Kinoshita, H. and Nosaka, T. (2005): Oceanographic data of the 43rd Japanese Antarctic Research Expedition from November 2001 to April 2002. JARE Data Rep., **282** (Oceanography 28), 63 p.

Le Traon, P.-Y., Nadal, F. and Ducet, N. (1998): An improved mapping method of multi-satellite altimeter data. J. Atmos. Oceanic Technol., **15**, 522–534.

Monterey, G. and Levitus, S. (1997): Seasonal Variability of Mixed Layer Depth for the World Ocean. NOAA Atlas NESDIS 14, U.S. Gov. Printing Office, Washington, D.C., 96 p. 87 figs.

Odate, T., Kudoh, S. and Fukuchi, M. (2001): Report on workshop "Planning of future science in the Antarctic Ocean study with cooperation among study groups". Nankyoku Shiryô (Antarct. Rec.), **45**, 362–370 (in Japanese with English abstract).

Orsi, A.H., Whitworth, T. and Nowlin, W.D. (1995): On the meridional extent and fronts of the Antarctic Circumpolar Current. Deep. Sea Res., **42**, 641–673.

Rintoul, S.R. and Bullister, J.L. (1999): A late winter hydrographic section from Tasmania to Antarctica. Deep-Sea Res. I, **46**, 1417–1454.

Rintoul, S.R., Donguy, J.-R. and Roemmich, D.H. (1997): Seasonal evolution of upper ocean thermal structure between Tasmania and Antarctica. Deep-Sea Res. I, **44**, 1185–1202.

Rosenberg, M., Rintoul, S., Bray, S., Curran, C. and Johnston, N. (2005): Aurora Australis Marine Science Cruise AU0103, CLIVAR-SR3 Transect-Oceanographic Field Measurements and Analysis. Hobart, ACE-CRC, unpublished report.

Sokolov, S. and Rintoul, S.R. (2002): Structure of Southern Ocean fronts at 140°E. J. Mar. Sys., **37**, 151–184.

Talley, L.D. (1999): Some aspects of ocean heat transport by the shallow, intermediate and deep overturning circulations. Mechanisms of Global Climate Change at Millennial Time Scales, ed. by P.U. Clark *et al.* Washington, D.C., Am. Geophys. Union, 1–22 (AGU. Geophys. Mono. Ser., **112**).

Trull, T., Rintoul, S.R., Hadfield, M. and Abraham, E.R. (2001): Circulation and seasonal evolution of polar waters south of Australia: implications for iron fertilization of the Southern Ocean. Deep-Sea Res. II, **48**, 2439–2466.

Whitworth, T., Orsi, A.H., Kim, S.-J. and Nowlin, W.D. (1998): Water masses and mixing near the Antarctic Slope Front. Ocean, Ice and Atmosphere: Interactions at Antarctic Continental Margin, ed. by S.S. Jacobs and R. Weiss. Washington, D.C., Am. Geophys. Union, 1–27 (Antarct. Res. Ser., **75**).

Worby, A.P., Massom, R.A., Allison, I., Lytle, V.I. and Heil, P. (1998): East Antarctic sea ice: A review of its structure, properties and drift. Antarctic Sea Ice: Physical Processes, Interactions and Variability, ed. by M.O. Jeffries. Washington, D.C., Am. Geophys. Union, 41–67 (Antarct. Res. Ser., **74**).